



# Risk analysis in peripheral clinical T1 non-small cell lung cancer correlations between tumor-to-blood standardized uptake ratio on $^{18}\text{F}$ -FDG PET-CT and primary tumor pathological invasiveness: a real-world observational study

Xiao-Feng Li<sup>1,2</sup>, Yun-Mei Shi<sup>1</sup>, Rong Niu<sup>1</sup>, Xiao-Nan Shao<sup>1</sup>, Jian-Feng Wang<sup>1</sup>, Xiao-Liang Shao<sup>1</sup>, Fei-Fei Zhang<sup>1</sup>, Yue-Tao Wang<sup>1,3</sup>

<sup>1</sup>Department of Nuclear Medicine, The Third Affiliated Hospital of Soochow University, Changzhou, China; <sup>2</sup>Department of Radiology, Xuzhou Cancer Hospital, Xuzhou, China; <sup>3</sup>Changzhou Key Laboratory of Molecular Imaging, Changzhou, China

**Contributions:** (I) Conception and design: YT Wang, XF Li; (II) Administrative support: YT Wang, XF Li; (III) Provision of study materials or patients: XF Li, YM Shi; (IV) Collection and assembly of data: XF Li, YM Shi, R Niu; (V) Data analysis and interpretation: XF Li, XL Shao; (VI) Manuscript writing: All authors; (VII) Final approval of manuscript: All authors.

**Correspondence to:** Yue-Tao Wang, MD. Department of Nuclear Medicine, The Third Affiliated Hospital of Soochow University, No. 185, Juqian Street, Changzhou, China. Email: yuetao-w@163.com.

**Background:** Sublobar resection is not suitable for patients with pathological invasiveness [including lymph node metastasis (LNM), visceral pleural invasion (VPI), and lymphovascular invasion (LVI)] of peripheral clinical T1 (cT1) non-small cell lung cancer (NSCLC), while primary tumor maximum standardized uptake value ( $\text{SUV}_{\text{max}}$ ) on  $^{18}\text{F}$ -FDG PET-CT is related to pathological invasiveness, the significance differed among different institutions is still challenging. This study explored the relationship between the tumor-to-blood standardized uptake ratio (SUR) of  $^{18}\text{F}$ -FDG PET-CT and primary tumor pathological invasiveness in peripheral cT1 NSCLC patients.

**Methods:** This retrospective study included 174 patients with suspected lung neoplasms who underwent preoperative  $^{18}\text{F}$ -FDG PET-CT. We compared the differences of the clinicopathological variables, metabolic and morphological parameters in the pathological invasiveness and less-invasiveness group. We performed a trend test for these parameters based on the tertiles of SUR. The relationship between SUR and pathological invasiveness was evaluated by univariate and multivariate logistics regression models (included unadjusted, simple adjusted, and fully adjusted models), odds ratios (ORs), and 95% confidence intervals (95% CIs) were calculated. A smooth fitting curve between SUR and pathological invasiveness was produced by the generalized additive model (GAM).

**Results:** Thirty-eight point five percent of patients had pathological invasiveness and tended to have a higher SUR value than the less-invasiveness group [6.50 (4.82–11.16) vs. 4.12 (2.04–6.61),  $P < 0.001$ ]. The trend of  $\text{SUV}_{\text{max}}$ , mean standardized uptake value ( $\text{SUV}_{\text{mean}}$ ), metabolic tumor volume (MTV), total lesion glycolysis (TLG), mean CT value ( $\text{CT}_{\text{mean}}$ ), size of the primary tumor, neuron-specific enolase (NSE), the incidence of LNM, adenocarcinoma (AC), and poor differentiation in the tertiles of SUR value were statistically significant ( $P$  were  $< 0.001$ ,  $< 0.001$ , 0.010,  $< 0.001$ ,  $< 0.001$ , 0.002, 0.033,  $< 0.001$ , 0.002, and  $< 0.001$ , respectively). Univariate analysis showed that the risk of pathological invasiveness increased significantly with increasing SUR [OR: 1.13 (95% CI: 1.06–1.21),  $P < 0.001$ ], and multivariate analysis demonstrated SUR, as a continuous variable, was still significantly related to pathological invasiveness [OR: 1.09 (95% CI: 1.01–1.18),  $P = 0.032$ ] after adjusting for confounding covariates. GAM revealed that SUR tended to be linearly and positively associated with pathological invasiveness and E-value analysis suggested robustness to unmeasured confounding.

**Conclusions:** SUR is linearly and positively associated with primary tumor pathological invasiveness independent of confounding covariates in peripheral cT1 NSCLC patients and could be used as a supplementary risk maker to assess the risk of pathological invasiveness.

**Keywords:** Non-small cell lung cancer (NSCLC); PET-CT; risk factor; odds ratio (OR)

Submitted Apr 12, 2021. Accepted for publication Jun 09, 2021.

doi: 10.21037/qims-21-394

View this article at: <https://dx.doi.org/10.21037/qims-21-394>

## Introduction

Surgical resection remains the primary and preferred approach for the treatment of early-stage lung cancer (1), especially for clinical T1 (cT1) non-small cell lung cancer (NSCLC). Sublobar resection, such as segmentectomy or wedge resection, may be of greater benefit according to the 3<sup>rd</sup> edition of the American College of Chest Physicians (ACCP) guidelines (2). The JCOG0201 (3) clinical trial (Japan Clinical Oncology Group Study) also verified that segmentectomy for peripheral clinical stage IA (cT1N0M0) NSCLC had a similar local-control and 10-year survival rate (4) and surgical safety (5) compared to lobectomy. However, for patients with clinical stage IA NSCLC who underwent sublobar resection, visceral pleural invasion (VPI) and lymphovascular invasion (LVI) were recognized as independent predictors of locoregional recurrence and poor disease-specific survival. Based on this, Koike *et al.* (6) concluded that patients without VPI and LVI might be candidates for sublobar resection, and the determination of a reliable risk marker for pathological invasiveness [such as lymph node metastasis (LNM), VPI, or LVI] could provide a decision-making basis for peripheral cT1 NSCLC patients.

Katsumata (7) has proposed that the maximum solid component diameter divided by the maximum tumor diameter of  $\leq 0.5$  can predict pathological less-invasiveness (without nodal involvement or vessel invasion) in lung cancer from CT scans. However, precise measurement of the solid component in CT often differs between observers.  $^{18}\text{F}$ -FDG PET-CT integrates anatomical and metabolic information and has been recommended for staging NSCLC (2), and some studies on patients with peripheral cT1 NSCLC have described the relationship between maximum standardized uptake value ( $\text{SUV}_{\text{max}}$ ) on  $^{18}\text{F}$ -FDG PET-CT with pathological tumor invasiveness (8,9). Tsutani *et al.* (8) showed that this demonstrated pathologic less-invasiveness when the primary tumor  $\text{SUV}_{\text{max}} \leq 1.5$ . However, the measurement of  $\text{SUV}_{\text{max}}$  had been affected

by some well-known factors such as uptake interval, reconstruction protocol, and equipment that vary among institutions (10).

Recently, Yang and colleagues (11) have found that the influx-rate constant ( $K_i$ ) based on dynamic modeling showed more sensitivity than SUV to detect LNM in NSCLC, and van den Hoff (12) has clearly shown that the tumor-to-blood standardized uptake ratio (SUR) was a substitute for  $K_i$  in  $^{18}\text{F}$ -FDG. However, real-world evidence is scarce regarding the correlation between SUR and pathological invasiveness in peripheral cT1 NSCLC. Our research hypothesized that primary tumor SUR might be used to stratify peripheral cT1 NSCLC by pathological invasiveness and explored the dose-effect relationship.

## Methods

### Study population and data collection

This retrospective study enrolled 174 consecutive patients with suspected lung neoplasms who underwent preoperative  $^{18}\text{F}$ -FDG PET-CT in the Third Affiliated Hospital of Soochow University between January 2017 and March 2020. Patients were eligible for inclusion if they met the following criteria: (I) the cT1 pulmonary lesions were staged by the 8<sup>th</sup> edition of the American Joint Committee on Cancer (AJCC) staging system (13), and the peripheral tumor was defined as a lesion located in the outer two-thirds of the axial CT image (14). (II) The pathological diagnosis presented with adenocarcinoma (AC) or squamous cell carcinoma (SCC). (III) The number of lymph nodes (LNs) resected was  $\geq 6$  (according to the 8<sup>th</sup> edition of the AJCC staging system) (13). (IV) The time from  $^{18}\text{F}$ -FDG PET-CT to surgical resection was  $\leq 1$  month. The exclusion criteria for the study were any of the following: (I) the maximum diameter of the primary lesion was  $> 3$  cm on the CT axial lung window image. (II) Treatment with antitumor therapy, such as radiotherapy, chemotherapy,

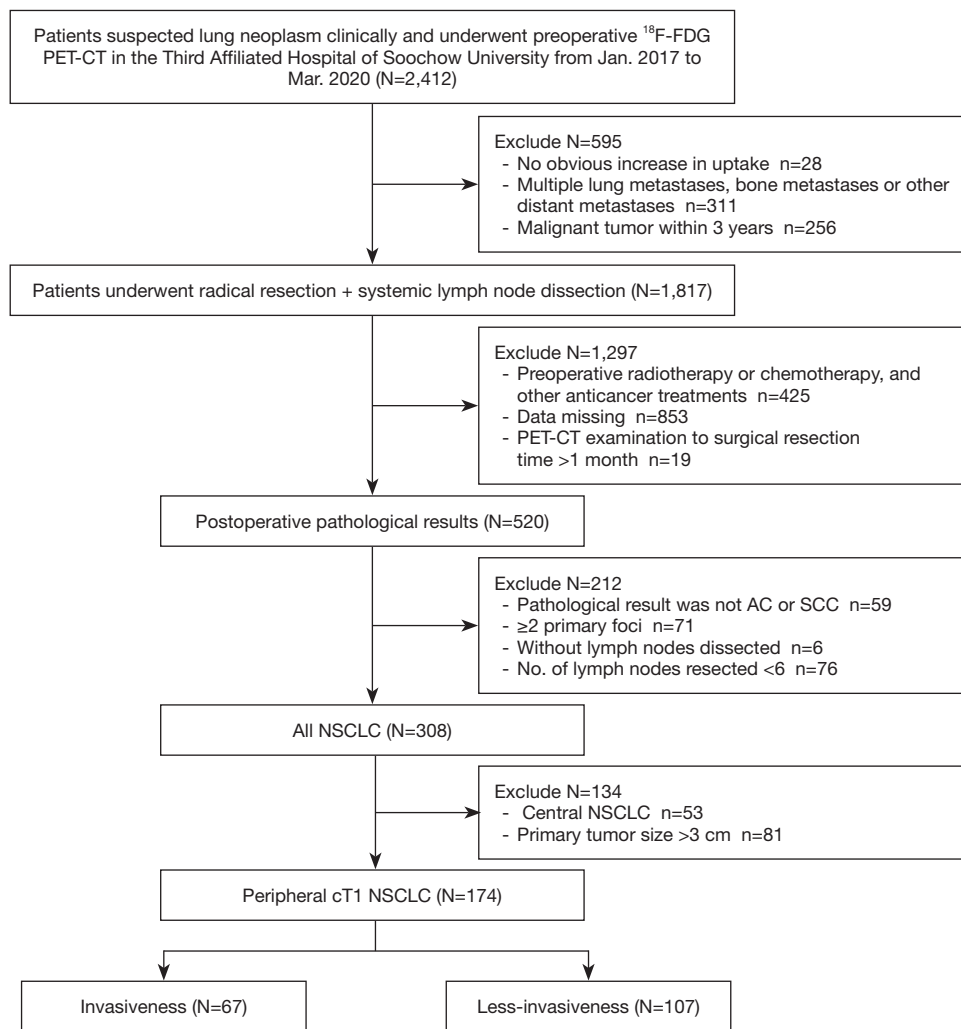


**Figure 1** Flow chart of the population selection. AC, adenocarcinoma; SCC, squamous cell carcinoma; NSCLC, non-small cell lung cancer; cT1, clinical T1.

targeted therapy, and immunity therapy, before surgery. (III) Multiple primary lung cancers ( $\geq 2$ ) confirmed by surgery or pathology and multiple lung metastases, bone metastases, or other distant metastasis by  $^{18}\text{F}$ -FDG PET-CT diagnosis or pathological confirmation. (IV) A history of cancer within the previous 3 years. *Figure 1* shows the flow chart of the population selection. We took the pathological invasiveness of the primary tumor as the primary study endpoint and defined it as one or more of LNM, VPI, and LVI confirmed by pathology. Less-invasiveness was defined as other conditions without these features, and we deemed the primary lesion SUR as the exposure factor. Risk factors reported in previous literature, including gender, age, body mass index (BMI), smoking status, primary tumor  $\text{SUV}_{\text{max}}$ ,

primary tumor mean standardized uptake value ( $\text{SUV}_{\text{mean}}$ ), primary tumor metabolic tumor volume (MTV), primary tumor total lesion glycolysis (TLG), mediastinal blood pool mean standardized uptake value ( $\text{MBP\_SUV}_{\text{mean}}$ ), primary tumor mean CT value ( $\text{CT}_{\text{mean}}$ ), primary tumor size (size), primary tumor location, histology, grade, number of LN dissections, and tumor immune markers [including CYFRA21-1, neuron-specific enolase (NSE), SCC] were considered as potential confounding covariates into our study. Information on gender, age, height, weight, smoking status, tumor immune markers (CYFRA21-1, NSE, SCC), and surgical procedure were extracted from patients' records, and the height and weight were collected to calculate BMI. Smoking status was recorded as never for

never having smoked or having quit smoking for more than 10 years, and ever for all other conditions. The study was conducted in accordance with the Declaration of Helsinki (as revised in 2013). The ethics committee approved the study protocol, and the requirement for informed consent was waived since the study was retrospective.

### *PET/CT scan*

Before the  $^{18}\text{F}$ -FDG PET-CT examination, all patients fasted for at least 6 hours, and the serum glucose levels were required to be  $\leq 10.0$  mmol/L before  $^{18}\text{F}$ -FDG was injected. Approximately 60 minutes after the intravenous injection of 4.44 MBq/kg  $^{18}\text{F}$ -FDG with radiochemical purity  $>95\%$ , we performed an examination from the skull to the upper thigh on a Siemens Biograph mCT 64 PET-CT instruments (Siemens Medical Solutions, Hoffman Estates, IL, USA) with the following parameters: 100 kV, 80 mA, tube rotation time, 0.5 seconds, pitch, 0.8; and 5 mm thickness. A PET scan was performed using a three-dimensional acquisition mode with a 2 minute/bed position that matched the CT section thickness and reconstructed using the ordered subset expectation maximization method (two iterations, 21 subsets, 2 mm full width at half maxima Gaussian filter) (15). Following this, all patients immediately underwent a breath-holding CT examination with the following parameters: 140 kV, 64 mAs; rotation time, 0.5 s; pitch, 0.6; slice thickness, 5.0 mm; and matrix, 512 $\times$ 512. The reconstruction algorithms included the B70f kernel, B41f kernel with lung window [window width (WW), 1,200 Hu; window level (WL), -600 Hu], and mediastinal window (WW, 250 Hu; WL, 40 Hu).

### *Measurement of metabolic and morphological parameters*

Two nuclear medicine physicians (XF Li with 12 years of experience and R Niu with 13 years of experience) were blinded to the clinical information and independently analyzed and measured the  $\text{SUV}_{\text{max}}$ ,  $\text{SUV}_{\text{mean}}$ , MTV, TLG, and  $\text{MBP\_SUV}_{\text{mean}}$  on the PET image and size,  $\text{CT}_{\text{mean}}$  on the CT image using Syngo TrueD software, Siemens Medical Systems workstation (see *Figure 2*). The MTV was calculated with 40%  $\text{SUV}_{\text{max}}$  as the contour line (16), and the TLG was calculated as  $\text{SUV}_{\text{mean}} \times \text{MTV}$ . A volume of interest (VOI) consisting of  $\geq 5$  cm<sup>3</sup> was manually drawn at the thoracic aorta on the CT sagittal image of the mediastinal window and had to avoid the calcification on the vascular wall. The  $\text{SUV}_{\text{mean}}$  of each VOI was measured as

the  $\text{MBP\_SUV}_{\text{mean}}$  (17), and the calculation of the primary tumor SUR was equal to the  $\text{SUV}_{\text{max}}$  divided by  $\text{MBP\_SUV}_{\text{mean}}$ . The maximum diameter of the primary tumor was measured on the axial CT image of the mediastinal window. The  $\text{CT}_{\text{mean}}$  was measured by the same size regions of interest (ROIs) at three different parts in the largest diameter of the primary tumor on the CT axial mediastinal window images, and the mean value of the three ROIs was calculated.

### *Surgical resection and pathological evaluation*

All patients underwent thoracotomy or video-assisted thoracoscopic surgery by radical resection with LN dissection. Radical resection included lobectomy, segmentectomy, or wedge resection, and LN dissection included systemic LN dissection. LNs were removed with the adipose connective tissue of the corresponding anatomic regions, as confirmed by the surgeon intraoperatively. After resection, the specimens were routinely fixed, embedded, sectioned, stained, and observed under a microscope at 200 $\times$  magnification to obtain a pathological diagnosis based on the World Health Organization classification of NSCLC (18). All resected LNs were analyzed microscopically with hematoxylin-eosin (HE) stain for metastatic infiltration, and VPI was considered positive when tumor cells extended beyond the elastic layer of the pleura, as determined by elastic staining. LVI was positive when tumor cells appeared in the lymphatic lumen and blood vessel, respectively (19). Hilar and mediastinal LN division referred to the IASLC LN map (20).

### *Statistical methods*

Continuous variables with a normal distribution were described as mean  $\pm$  SD, and a nonnormal distribution was listed as median with interquartile range. Categorical variables were displayed with integers and proportions, and normality was assessed for each variable by the Kolmogorov-Smirnov test. The Student's *t*-test was used in normally distributed continuous variables, and the Wilcoxon-Mann-Whitney U test was used in nonnormal distribution variables to determine differences. The chi-square test or Fisher's exact test was used for the comparison of categorical variables. The statistically different variables between the less-invasiveness and invasiveness groups were then analyzed. The SUR values were divided into three equal parts according to the sample distribution and defined as bottom

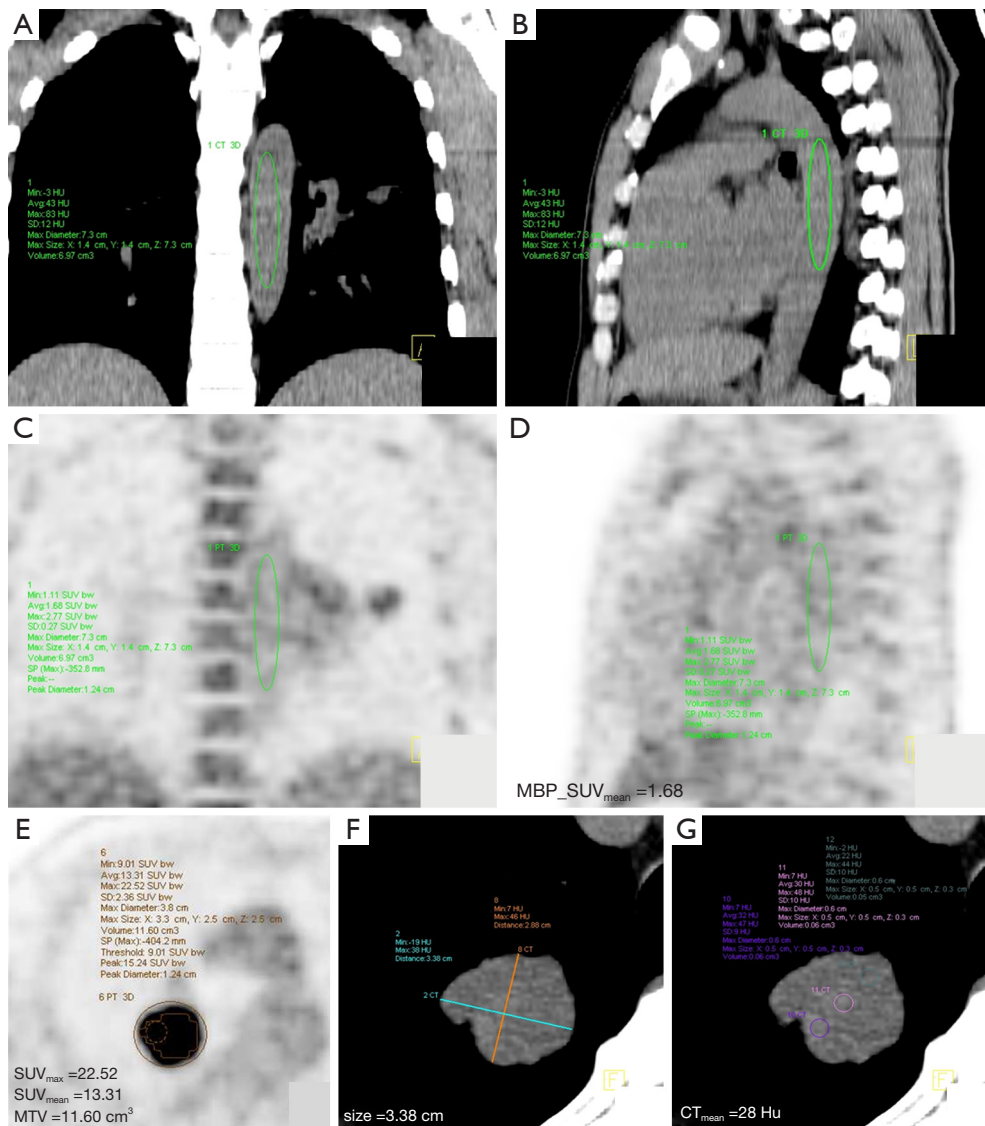


**Figure 2** Example of the thoracic aorta VOI definition. (A,B) were the coronal and sagittal images of the mediastinal window. (C,D) were the coronal and sagittal images of the PET image, respectively. The VOI consisting of  $\geq 5 \text{ cm}^3$  was manually drawn at the thoracic aortic on the CT sagittal image of the mediastinal window and had to avoid the calcification on the vascular wall. The  $\text{SUV}_{\text{mean}}$  of the VOI was the  $\text{MBP\_SUV}_{\text{mean}}$ . (E) showed the PET axis images to measure  $\text{SUV}_{\text{max}}$ ,  $\text{SUV}_{\text{mean}}$  and the irregular solid line on the inside represented taking the 40%  $\text{SUV}_{\text{max}}$  as the contour line to measure MTV ( $\text{SUV}_{\text{max}}$ ,  $\text{SUV}_{\text{mean}}$  and MTV were 22.52, 13.31, and  $11.60 \text{ cm}^3$ , respectively). (F) showed the maximum diameter of the lesion on the CT axial mediastinal window image (size = 3.38 cm). (G) showed the same size ROIs (ROI1, ROI2, and ROI3) on the maximum diameter of the primary lesion on the CT axial image,  $\text{CT}_{\text{mean}} = (\text{ROI1} + \text{ROI2} + \text{ROI3})/3$  ( $\text{CT}_{\text{mean}} = 28 \text{ Hu}$ ). VOI, volume of interest;  $\text{SUV}_{\text{mean}}$ , mean standardized uptake value;  $\text{MBP\_SUV}_{\text{mean}}$ , mediastinal blood pool mean standardized uptake value; MTV, metabolic tumor volume;  $\text{SUV}_{\text{max}}$ , maximum standardized uptake value; ROI, region of interest.

tertile, middle tertile, and high tertile. A trend test evaluated the covariates related to tertiles of SUR. Covariates were included as potential confounders in the final models if they either changed SUR estimates on pathological tumor

invasiveness by more than 10% or were significantly associated with pathological tumor invasiveness (21). A variance inflation factor (VIF)  $\leq 5$  was calculated using a simple linear regression model to avoid the collinearity

issue. Finally, three models (unadjusted, simple adjusted, and fully adjusted) were established using multivariate logistic regression analysis. Model I was a univariable logistic regression with unadjusted factors, model II adjusted for age and gender, and model III adjusted for age, gender, BMI, and other confounding factors. The odds ratios (ORs) and 95% confidence intervals (95% CIs) of SUR in different models were then calculated. The generalized additive model (GAM) describes the relationship between SUR and pathological invasiveness by a smooth fitting curve. We explored the potential for unmeasured confounding by calculating E-values (22), where the E-value quantified the required magnitude of an unmeasured confounder that could negate the observed association between SUR and pathological tumor invasiveness. We then utilized the interclass correlation coefficient (ICC) to determine the agreement in feature values between the observers in 30 randomly selected patients (23).

Analyses were performed with R software (version 3.4.3, <https://www.r-project.org>, R packages: glmnet, pROC, rms, and dca. R). All P values were two-tailed, with a P value of less than 0.05 indicating statistical significance.

## Results

The number and proportion of males and females among the enrolled patients were 77 (44.3%) and 97 (55.7%), respectively. A total of 67 (38.5%) patients had pathological invasiveness of the primary tumor, and LNM, VPI, and LVI were evident in 43 (24.7%), 28 (16.1%), and 11 (6.3%) patients, respectively. There were also had seven patients with LNM and VPI, five patients with LNM and LVI, two patients with VPI and LVI, and one patient with LNM, VPI, and LVI. Primary tumors were located in the right upper lobe in 74 cases, the right middle lobe in 10 cases, the right lower lobe in 38 cases, the left upper lobe in 37 cases, and the left lower lobe in 15 cases. The inter-observer ICCs and 95% CIs of the  $SUV_{max}$ ,  $MBP\_SUV_{mean}$ , and MTV were 0.995 (0.989–0.998), 0.995 (0.990–0.999) and 0.994 (0.989–0.997), respectively, whereas the intra-observer ICC were 0.994 (0.987–0.997), 0.985 (0.968–0.993) and 0.994 (0.988–0.997), respectively. The range of the ICC values was 0.985–0.995, which indicates high reliability and reproducibility.

### *Baseline characteristics of pathological invasiveness and less-invasiveness tumors*

The baseline characteristics of the study population

between the pathological tumor invasiveness group and the less-invasiveness group are shown in *Table 1*. The SUR value in the pathological invasiveness group was higher than the less-invasiveness group, and the difference had statistical significance (P value <0.001). *Table 1* also shows that the differences of  $SUV_{max}$ ,  $SUV_{mean}$ , TLG,  $CT_{mean}$ , size, and grade between the two groups were statistically significant (P values were <0.001, <0.001, 0.001, 0.015, 0.016, and <0.001, respectively). With the increase of SUR value, the number and proportion of primary tumor pathological invasiveness also increased correspondingly. The number and proportion in the bottom, middle, and high tertile were 12 (20.7%), 22 (37.9%), and 33 (56.9%), respectively (P for trend <0.001). The results of univariate logistic regression analysis for other variables except SUR are also shown in *Table 1*. The baseline characteristics stratified by tertiles of SUR value are shown in *Table 2*. The trend of  $SUV_{max}$ ,  $SUV_{mean}$ , MTV, TLG,  $CT_{mean}$ , size, and NSE, and the incidence of LNM, AC and poor differentiation, in the tertiles of SUR values were statistically significant (P values were <0.001, <0.001, 0.01, <0.001, <0.001, 0.002, 0.033, <0.001, <0.001, and 0.002, respectively).

### *Univariable logistic regression analysis between SUR and pathological invasiveness*

A univariate analysis (*Table 3*) showed that the OR values for pathological invasiveness progressively increased across SUR tertiles. When SUR was used as a continuous variable, its OR value was 1.13 (95% CI: 1.06–1.21) and P value <0.001, and when SUR was used as a categorical variable, the OR value for pathological invasiveness was 5.06 (95% CI: 2.23–11.50) and P value <0.001 in patients with a SUR in the top tertile compared to those in the bottom tertile. Additionally,  $SUV_{mean}$  and  $SUV_{max}$  did not enter the multiple regression model due to the collinearity issue with SUR.

### *Multivariate logistic regression analysis between SUR and pathological invasiveness and GAM analysis*

The multivariable logistic regression analysis also demonstrated a significant association between SUR and pathological invasiveness. In multivariate model II (adjusted for gender and age), the OR for invasiveness progressively increased across tertiles of SUR (P for trend <0.001) (*Table 3*), and a per-SD increase in SUR, the OR was 1.14 (95% CI: 1.06–1.22), P value <0.001. Multivariate model III (adjusted for gender, age, BMI,  $CT_{mean}$ , size, TLG, and grade) did

**Table 1** Baseline characteristics of the study population

Variables	Total (n=174)	OR (95% CI)	Less-invasiveness (n=107)	Invasiveness (n=67)	P value
SUR	5.16 (2.54–8.47)	–	4.12 (2.04–6.61)	6.50 (4.82–11.16)	<0.001
Male, n (%)	77 (44.3)	0.94 (0.51–1.74)	48 (44.9)	29 (43.3)	0.839
Age, years	63.12±7.86	0.99 (0.95–1.03)	63.29±8.19	62.85±7.35	0.772
BMI, kg/m <sup>2</sup>	23.75±2.93	1.00 (0.90–1.11)	23.75±2.94	23.74±2.94	0.996
Active smoking, n (%)	42 (24.1)	1.27 (0.63–2.57)	24 (22.4)	18 (26.9)	0.506
SUV <sub>max</sub>	7.20 (3.60–12.18)	1.09 (1.03–1.14)	5.50 (3.15–9.55)	9.30 (6.35–15.15)	<0.001
SUV <sub>mean</sub>	4.45 (2.08–7.55)	1.14 (1.06–1.24)	3.10 (1.85–5.55)	5.90 (3.75–9.10)	<0.001
MTV, mL	3.20 (1.80–5.93)	1.03 (0.95–1.11)	3.20 (1.75–5.15)	3.20 (2.20–6.80)	0.461
TLG	14.00 (7.55–27.10)	1.02 (1.01–1.04)	10.80 (6.15–19.50)	19.70 (10.95–40.10)	<0.001
MBP_SUV <sub>mean</sub>	1.44 (1.26–1.68)	0.45 (0.16–1.23)	1.47 (1.31–1.68)	1.39 (1.19–1.60)	0.083
CT <sub>mean</sub> , Hu	20.17 (–21.58 to 29.33)	1.01 (1.00–1.01)	17.00 (–57.84 to 28.66)	23.00 (14.50–30.16)	0.015
Size, cm	2.35 (1.80–2.63)	2.08 (1.19–3.61)	2.20 (1.70–2.50)	2.50 (2.00–3.00)	0.016
Right lung, n (%)	122 (70.1)	0.89 (0.46–1.74)	76 (71.0)	46 (68.7)	0.739
CYFRA21-1	2.96 (2.23–2.98)	1.17 (0.86–1.59)	2.96 (2.17–2.96)	2.96 (2.33–3.19)	0.295
NSE	12.23 (11.63–14.94)	1.01 (0.96–1.06)	12.23 (11.23–14.54)	12.23 (11.93–15.82)	0.183
SCC	0.80 (0.70–1.00)	1.23 (0.86–1.76)	0.80 (0.65–1.00)	0.80 (0.80–0.98)	0.524
Poor differentiation, n (%)	60 (34.5)	5.70 (2.89–11.27)	21 (19.6)	39 (58.2)	<0.001
AC, n (%)	159 (91.4)	0.93 (0.32–2.75)	98 (91.6)	61 (91.0)	0.901
Surgical procedure, n (%)					0.292
Lobectomy	130 (74.7)	1	77 (72.0)	53 (79.1)	
Sublobar resection	44 (25.3)	0.70 (0.30–1.40)	30 (28.0)	14 (20.9)	
Segmentectomy	27 (15.5)	–	21 (19.6)	6 (9.0)	
Wedge resection	17 (9.8)	–	9 (8.4)	8 (11.9)	

Continuous variables with a normal distribution were described as mean ± SD, and a nonnormal distribution was listed as median with interquartile range; categorical variables were displayed with integers and proportions. Invasiveness: including one or more VPI, LVI, and LNM. Less-invasiveness was defined as all other conditions without these features. OR, odds ratio; CI, confidence interval; SUR, primary tumor tumor-to-blood standardized uptake value ratio; BMI, body mass index; SUV<sub>max</sub>, primary tumor maximum standardized uptake value; SUV<sub>mean</sub>, the mean standardized uptake value; MTV, primary tumor metabolic tumor volume; TLG, primary tumor total lesion glycolysis; MBP\_SUV<sub>mean</sub>, the mediastinal blood pool mean standardized uptake value; CT<sub>mean</sub>, primary tumor mean CT value; size, primary tumor size; NSE, neuron-specific enolase; SCC, squamous cell carcinoma; AC, adenocarcinoma; VPI, visceral pleural invasion; LVI, lymphovascular invasion; LNM, lymph node metastasis.

not significantly alter the results. Consistent with these findings, multivariate analysis demonstrated that SUR, as a continuous variable, was still significantly related to pathological invasiveness [OR for per-SD: 1.09 (95% CI: 1.01–1.18), P value =0.032]. Finally, to further confirm the reliability of our results, we conducted a sensitivity analysis. The stratified analysis (Table 4) showed that the significant positive correlation of SUR for peripheral cT1 tumors

was consistent in AC, non-smokers, <65 years, and well/moderate differentiation patients, and the P values were all <0.05. However, in the poor differentiation subgroup, the ORs of the SUR in the middle and top tertile were 0.57 (0.09–3.83) and 0.80 (0.13–4.75), and they were not statistically significant (P=0.564, and 0.806, respectively).

GAM (Figure 3) was performed to visually assess the association between SUR and pathological invasiveness

**Table 2** Baseline characteristics stratified by tertiles of SUR (n=174)

Variables	Bottom tertile (n=58)	Middle tertile (n=58)	Top tertile (n=58)	P value for trend
SUR	1.94 (1.43–2.58)	5.16 (4.39–5.95)	11.29 (8.29–15.29)	
Male, n (%)	21 (36.2)	23 (39.7)	33 (56.9)	0.056
Age, years	63.67±7.13	63.19±9.14	62.50±7.24	0.623
BMI, kg/m <sup>2</sup>	24.19±2.80	23.81±2.92	23.26±3.04	0.178
Active smoking, n (%)	10 (17.2)	13 (22.4)	19 (32.8)	0.138
SUV <sub>max</sub>	3.05 (2.30–3.60)	7.40 (6.10–8.70)	15.85 (11.48–20.47)	<0.001
SUV <sub>mean</sub>	1.80 (1.33–2.10)	4.55 (3.62–5.40)	10.10 (7.00–12.30)	<0.001
MTV, mL	4.10 (2.30–8.95)	2.95 (1.85–4.68)	2.80 (1.70–4.30)	0.01
TLG	8.00 (3.92–16.12)	13.15 (8.77–21.15)	25.70 (15.18–48.22)	<0.001
MBP_SUV <sub>mean</sub>	1.56±0.32	1.47±0.28	1.37±0.32	0.069
CT <sub>mean</sub> , Hu	-48.84 (-192.75 to 16.67)	21.50 (11.92–31.00)	25.84 (19.08–30.33)	<0.001
Size, cm	2.00 (1.50–2.50)	2.50 (2.00–3.00)	2.50 (2.00–2.68)	0.002
Right lung, n (%)	42 (72.4)	41 (70.7)	39 (67.2)	0.825
CYFRA21-1	2.96 (2.04–2.96)	2.96 (2.48–3.15)	2.96 (2.39–2.96)	0.368
NSE	12.23 (11.29–13.47)	12.23 (11.27–14.39)	12.77 (12.23–16.29)	0.033
SCC	0.80 (0.60–0.90)	0.80 (0.70–1.00)	0.80 (0.80–1.10)	0.177
LNM, n (%)	5 (8.6)	13 (22.4)	25 (43.1)	<0.001
VPI, n (%)	7 (12.1)	13 (22.4)	8 (13.8)	0.267
LVI, n (%)	3 (5.2)	5 (8.6)	3 (5.2)	0.678
Poor differentiation, n (%)	7 (12.1)	17 (29.3)	36 (62.1)	<0.001
AC, n (%)	57 (98.3)	55 (94.8)	47 (81.0)	0.002
Invasivness, n (%)	12 (20.7)	22 (37.9)	33 (56.9)	<0.001

Continuous variables with a normal distribution were described as mean ± SD, and a nonnormal distribution was listed as median with interquartile range; categorical variables were displayed with integers and proportions. SUR, primary tumor tumor-to-blood standardized uptake value ratio; BMI, body mass index; SUV<sub>max</sub>, primary tumor maximum standardized uptake value; SUV<sub>mean</sub>, the mean standardized uptake value; MTV, primary tumor metabolic tumor volume; TLG, primary tumor total lesion glycolysis; MBP\_SUV<sub>mean</sub>, the mediastinal blood pool mean standardized uptake value; CT<sub>mean</sub>, primary tumor mean CT value; size, primary tumor size; NSE, neuron-specific enolase; SCC, squamous cell carcinoma; LNM, lymph node metastasis; VPI, visceral pleural invasion; LVI, lymph vascular invasion; AC, adenocarcinoma.

after adjusting for gender, age, BMI, CT<sub>mean</sub>, size, TLG, and grade, and the smooth fitting curve showed that SUR tended to be linearly associated with pathological invasiveness. We generated an E-value to assess the sensitivity to unmeasured confounding, and the primary findings were robust. For unmeasured confounding, which might change our results that SUR was significantly related to pathological invasiveness would be unlikely (E-value =1.26).

## Discussion

The main findings of this research were as follows: (I) compared with pathological less-invasiveness of peripheral cT1 NSCLC patients, individuals with pathological invasiveness had a higher value of SUR, as well as a higher value of TLG, size, and CT<sub>mean</sub>. (II) With the increase of SUR, TLG and the proportion of LNM increased, while MTV and the proportion of AC decreased. (III)

**Table 3** Multivariate regression analysis for the dose-effect relationship of SUR on pathological invasiveness

Exposure	Model I, OR (95% CI), P	Model II, OR (95% CI), P	Model III, OR (95% CI), P
SUR (per-SD)	1.13 (1.06–1.21), <0.001	1.14 (1.06–1.22), <0.001	1.09 (1.01–1.18), 0.032
Tertiles			
Bottom tertile	1	1	1
Middle tertile	2.34 (1.02–5.36), 0.044	2.38 (1.04–5.46), 0.041	1.71 (0.68–4.28), 0.252
Top tertile	5.06 (2.23–11.50), <0.001	5.47 (2.35–12.72), <0.001	3.36 (1.23–9.18), 0.012
P value for trend	<0.001	<0.001	0.017

Model I adjust for none; model II adjust for gender, age; model III adjust for gender, age, BMI, CT<sub>mean</sub>, size, TLG, and grade. SUR, primary tumor tumor-to-blood standardized uptake value ratio; BMI, body mass index; CT<sub>mean</sub>, primary tumor mean CT value; size, primary tumor size; TLG, primary tumor total lesion glycolysis.

**Table 4** Stratified analysis with the grade, gender, age, smoking status, and histology subgroup

Variables	N	Bottom tertile	Middle tertile, OR (95% CI), P	Top tertile, OR (95% CI), P
Grade				
Well/moderate	114	1	2.60 (0.92–7.38), 0.073	4.35 (1.36–13.96), 0.013
Poor	60	1	0.57 (0.09–3.83), 0.564	0.80 (0.13–4.75), 0.806
Gender				
Female	97	1	2.07 (0.75–5.70), 0.157	4.67 (1.56–13.98), 0.006
Male	77	1	3.20 (0.72–14.25), 0.127	7.20 (1.77–29.23), 0.006
Age				
<65 years	96	1	3.29 (1.05–10.30), 0.041	3.78 (1.24–11.50), 0.019
≥65 years	78	1	1.54 (0.45–5.25), 0.487	8.38 (2.36–29.74), 0.001
Smoking status				
Never	132	1	2.78 (1.11–6.93), 0.029	4.00 (1.57–10.22), 0.004
Ever	42	1	1.20 (0.16–9.01), 0.859	8.67 (1.39–53.85), 0.021
Histology				
SCC	15	1	&	&
AC	159	1	2.50 (1.09–5.76), 0.031	5.06 (2.14–11.97), <0.001

&, the statistics failed because of the small sample size. SCC, squamous cell carcinoma; AC, adenocarcinoma.

Multivariable logistic regression analysis revealed SUR was positively associated with pathological invasiveness independent of confounding factors. GAM indicated that SUR was linearly associated with the risk of pathological invasiveness.

In a multi-center observational study of 10,885 Chinese populations (24), VPI and LVI were risk factors for N2 LNM with cT1 NSCLC patients, and peripheral cT1 NSCLC with VPI and LVI prompted a poor prognosis.

Zhang *et al.* (25) proved that the overall 3-year survival rate for peripheral cT1 NSCLC patients with VPI was 71.7%. In addition, Tao (26) also confirmed that a primary tumor with LVI reflected a poor prognosis in peripheral cT1 NSCLC, and the overall 5-year survival rate was only 66.7%. However, for peripheral cT1 NSCLC patients, how to describe the risk of the VPI, LVI, and LNM of the primary tumor is still challenging. A previous study (27) used 3D evaluations on CT images to predict the

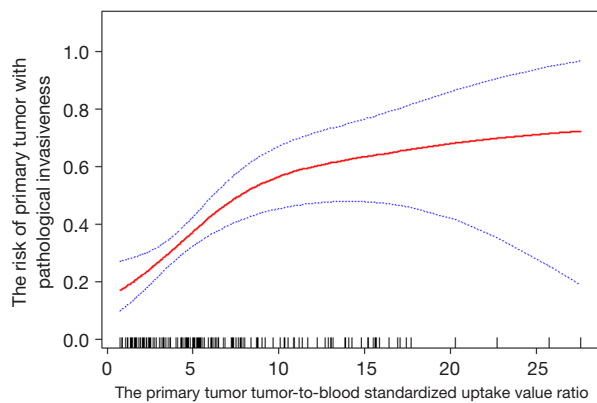


**Figure 3** The smooth fitting curve showed that SUR tended to be linearly associated with pathological invasiveness. The GAM showed SUR tended to be linearly associated with pathological invasiveness after adjusting for gender, age, BMI,  $CT_{mean}$ , size, TLG, and grade. The X-abcissa represented the SUR value, and the Y-ordinate represented the risk of primary tumor pathological invasiveness. The solid red line represented SUR was linearly associated with pathological invasiveness, and the blue dotted lines above and below represent the 95% CI. SUR, standardized uptake ratio; GAM, generalized additive model; BMI, body mass index;  $CT_{mean}$ , mean CT value; TLG, total lesion glycolysis; CI, confidence interval.

pathological LNM and tumor invasiveness of cT1N0M0 lung AC and found that solid tumor size was positively correlated with pathological invasiveness. However, the measurement of solid tumor size differed using different software and among the different observers (28,29).  $^{18}F$ -FDG PET-CT integrates anatomical and metabolic information and is currently the primary tool for staging NSCLC (30), and previous studies have demonstrated that  $SUV_{max}$  was related to VPI, LVI, and LNM. Tsutani *et al.* (31) reported that the  $SUV_{max}$  on  $^{18}F$ -FDG PET-CT helped predict pathological invasiveness in clinical stage IA lung AC and  $^{18}F$ -FDG uptake was closely related to solid tumor size. However, the stability and reproducibility of  $SUV_{max}$  were controversial and were affected by equipment type, acquisition method, and the reconstruction algorithm (10). Moreover, the study was flawed because of the use of univariable analysis biased by other significant confounders.

Recently, Jansen *et al.* (32) have validated that image-based SUR was an optimal trade-off between a reliable surrogate for the Ki of the tracer versus the simplicity of its assessment. In contrast, the SUV, normalized either to body weight or lean body mass, showed a poor Ki correlation.

Bütof *et al.* (17) also suggested that SUR improved the prognosis value in neoadjuvant radiochemotherapy esophageal cancer patients compared with conventional PET parameters. These results have led SUR to be investigated as a new potential parameter. Notably, there are few studies on the correlation analysis between SUR and peripheral cT1 NSCLC pathological invasiveness. Our study confirmed that SUR was higher in the peripheral cT1 NSCLC with pathological invasiveness and found that SUR was significantly and positively associated with pathological invasiveness by adjusting for confounding covariates. The stratified analysis showed that the OR values of SUR for pathological invasiveness in the middle and top tertile were 2.50 (1.09–5.76) and 5.06 (2.14–11.97) compared with the bottom tertile in AC, which proves that the positive correlation between SUR and primary tumor pathological invasiveness was more effective in peripheral cT1 lung AC. When analyzing the relationship between SUR and peripheral cT1 NSCLC pathological invasiveness by a GAM, we found that SUR was linearly associated with pathological invasiveness, suggesting that when it was higher, peripheral cT1 NSCLC patients were more likely to have pathological invasiveness. Furthermore, we suggested that radiochemotherapy or targeted therapy might be performed priority instead of surgery for these patients.

Additionally, we found that with increasing SUR, the number and proportion of SCC was 1 (1.7%), 3 (5.2%), and 11 (19.0%), respectively, which showed an increasing trend, while the proportion of AC was 57 (98.3%), 55 (94.8%), and 47 (81.0%), respectively, which showed a decreasing trend. These results demonstrated that with increasing SUR, the possibility that the lesion was AC was decreased, and the possibility that the lesion was SCC was increased in peripheral cT1 NSCLC. Our study also revealed that the difference of SUR value between AC and SCC was statistically significant in poor differentiation peripheral cT1 NSCLC ( $8.4 \pm 4.4$  vs.  $15.0 \pm 7.6$ ,  $P=0.006$ ), and poor differentiation SCC had a higher SUR. With the increasing trend of SUR, and when peripheral cT1 NSCLC had poor differentiation, a higher primary tumor  $CT_{mean}$ , larger primary tumor size, higher  $SUV_{max}$ ,  $SUV_{mean}$ , and TLG, the lesions probably had LNM, VPI, or LVI, and the number and proportion of LNM and TLG correspondingly increased. Although MTV, the number and proportion of AC have shown a decreasing trend, there was no statistical difference between the invasiveness and less-invasiveness groups. Therefore, we suggested that MTV and the number and proportion of AC were not confounding factors in our

risk analysis. Meanwhile, there was a statistical difference of  $SUV_{max}$  and  $SUV_{mean}$  between the tumor invasiveness and less-invasiveness groups, and it also increased with the increase of tertiles of SUR. However, we concluded a significant collinearity issue between  $SUV_{mean}$ ,  $SUV_{max}$  and SUR, since the Spearman analysis showed a strong correlation ( $r=0.96$ , and  $0.95$ , respectively)  $VIF=29.78$ , and  $24.44$ , respectively.

There are some limitations to our research, chiefly its retrospective nature and that we used a single-center cohort. Secondly, we used E-value analysis to quantify the potential implications of unmeasured confounders and found that the unmeasured confounders will not change the direction of our results. As the enrolled patients had resectable peripheral NSCLC, which might lead to the patient selection bias, this affected the subgroup with a larger SUR value. Thirdly, since the small sample size of SCC in the current study, the proportion of AC was 91.4%, which was similar to the results of the JCOG0201 study (3), our results are more applicable to AC rather than SCC. Another limitation of the real-world observational study was that, from the view of the long-term survival rate, it was not clear whether sublobectomy was suitable for resectable peripheral cT1 NSCLC with a low SUR value. We will discuss this issue in our future work.

## Conclusions

In this retrospective single-center study, SUR is linearly and positively associated with pathological invasiveness independent of confounding covariates and could be used as a supplementary risk marker to assess the risk of primary tumors pathological invasiveness in peripheral cT1 NSCLC. A large-scale multi-center prospective cohort study is needed to verify our results.

## Acknowledgments

*Funding:* This research was supported by grants from the National Natural Science Foundation of China (grant number: 81871381) and the Key Laboratory of Changzhou High-tech Research Project (grant number: CM20193010).

## Footnote

*Conflicts of Interest:* All authors have completed the ICMJE uniform disclosure form (available at <https://dx.doi.org/10.21037/qims-21-394>). The authors have no conflicts

of interest to declare.

*Ethical Statement:* The authors are accountable for all aspects of the work in ensuring that questions related to the accuracy or integrity of any part of the work are appropriately investigated and resolved. The study was conducted in accordance with the Declaration of Helsinki (as revised in 2013). The ethics committee approved the study protocol, and the requirement for informed consent was waived since the study was retrospective.

*Open Access Statement:* This is an Open Access article distributed in accordance with the Creative Commons Attribution-NonCommercial-NoDerivs 4.0 International License (CC BY-NC-ND 4.0), which permits the non-commercial replication and distribution of the article with the strict proviso that no changes or edits are made and the original work is properly cited (including links to both the formal publication through the relevant DOI and the license). See: <https://creativecommons.org/licenses/by-nc-nd/4.0/>.

## References

1. Howington JA, Blum MG, Chang AC, Balekian AA, Murthy SC. Treatment of stage I and II non-small cell lung cancer: diagnosis and management of lung cancer, 3rd ed: American College of Chest Physicians evidence-based clinical practice guidelines. *Chest* 2013;143:e278S-313S.
2. Silvestri GA, Gonzalez AV, Jantz MA, Margolis ML, Gould MK, Tanoue LT, Harris LJ, Detterbeck FC. Methods for staging non-small cell lung cancer: diagnosis and management of lung cancer, 3rd ed: American College of Chest Physicians evidence-based clinical practice guidelines. *Chest* 2013;143:e211S-50S.
3. Suzuki K, Koike T, Asakawa T, Kusumoto M, Asamura H, Nagai K, Tada H, Mitsudomi T, Tsuboi M, Shibata T, Fukuda H, Kato H ; Japan Lung Cancer Surgical Study Group (JCOG LCSSG). A prospective radiological study of thin-section computed tomography to predict pathological noninvasiveness in peripheral clinical IA lung cancer (Japan Clinical Oncology Group 0201). *J Thorac Oncol* 2011;6:751-6.
4. Nomori H, Mori T, Shiraishi A, Fujino K, Sato Y, Ito T, Suzuki M. Long-term prognosis after segmentectomy for cT1 N0 M0 non-small cell lung cancer. *Ann Thorac Surg* 2019;107:1500-6.
5. Suzuki K, Saji H, Aokage K, Watanabe SI, Okada M, Mizusawa J, Nakajima R, Tsuboi M, Nakamura S,

- Nakamura K, Mitsudomi T, Asamura H; West Japan Oncology Group; Japan Clinical Oncology Group. Comparison of pulmonary segmentectomy and lobectomy: Safety results of a randomized trial. *J Thorac Cardiovasc Surg* 2019;158:895-907.
6. Koike T, Koike T, Yoshiya K, Tsuchida M, Toyabe S. Risk factor analysis of locoregional recurrence after sublobar resection in patients with clinical stage IA non-small cell lung cancer. *J Thorac Cardiovasc Surg* 2013;146:372-8.
  7. Katsumata S, Aokage K, Nakasone S, Sakai T, Okada S, Miyoshi T, Tane K, Hayashi R, Ishii G, Tsuboi M. Radiologic criteria in predicting pathologic less invasive lung cancer according to TNM 8th edition. *Clin Lung Cancer* 2019;20:e163-70.
  8. Tsutani Y, Miyata Y, Nakayama H, Okumura S, Adachi S, Yoshimura M, Okada M. Prediction of pathologic node-negative clinical stage IA lung adenocarcinoma for optimal candidates undergoing sublobar resection. *J Thorac Cardiovasc Surg* 2012;144:1365-71.
  9. Kagimoto A, Tsutani Y, Izaki Y, Handa Y, Mimae T, Miyata Y, Okada M. Prediction of lymph node metastasis using semiquantitative evaluation of PET for lung adenocarcinoma. *Ann Thorac Surg* 2020;110:1036-42.
  10. Zhuang M, García DV, Kramer GM, Frings V, Smit EF, Dierckx R, Hoekstra OS, Boellaard R. Variability and repeatability of quantitative uptake metrics in 18F-FDG PET/CT of non-small cell lung cancer: impact of segmentation method, uptake interval, and reconstruction protocol. *J Nucl Med* 2019;60:600-7.
  11. Yang M, Lin Z, Xu Z, Li D, Lv W, Yang S, Liu Y, Cao Y, Cao Q, Jin H. Influx rate constant of 18F-FDG increases in metastatic lymph nodes of non-small cell lung cancer patients. *Eur J Nucl Med Mol Imaging* 2020;47:1198-208.
  12. van den Hoff J, Oehme L, Schramm G, Maus J, Lougovski A, Petr J, Beuthien-Baumann B, Hofheinz F. The PET-derived tumor-to-blood standard uptake ratio (SUR) is superior to tumor SUV as a surrogate parameter of the metabolic rate of FDG. *EJNMMI Res* 2013;3:77.
  13. Detterbeck FC, Boffa DJ, Kim AW, Tanoue LT. The eighth edition lung cancer stage classification. *Chest* 2017;151:193-203.
  14. Shin SH, Jeong DY, Lee KS, Cho JH, Choi YS, Lee K, Um SW, Kim H, Jeong BH. Which definition of a central tumour is more predictive of occult mediastinal metastasis in nonsmall cell lung cancer patients with radiological N0 disease? *Eur Respir J* 2019;53:1801508.
  15. Niu R, Shao X, Shao X, Jiang Z, Wang J, Wang Y. Establishment and verification of a prediction model based on clinical characteristics and positron emission tomography/computed tomography (PET/CT) parameters for distinguishing malignant from benign ground-glass nodules. *Quant Imaging Med Surg* 2021;11:1710-22.
  16. Kirienko M, Cozzi L, Rossi A, Voulaz E, Antunovic L, Fogliata A, Chiti A, Sollini M. Ability of FDG PET and CT radiomics features to differentiate between primary and metastatic lung lesions. *Eur J Nucl Med Mol Imaging* 2018;45:1649-60.
  17. Bütof R, Hofheinz F, Zöphel K, Schmollack J, Jentsch C, Zschaek S, Kotzerke J, van den Hoff J, Baumann M. Prognostic value of SUR in patients with trimodality treatment of locally advanced esophageal carcinoma. *J Nucl Med* 2018. [Epub ahead of print]. doi: 10.2967/jnumed.117.207670.
  18. Travis WD, Brambilla E, Nicholson AG, Yatabe Y, Austin JHM, Beasley MB, et al. The 2015 World Health Organization Classification of lung tumors: impact of genetic, clinical and radiologic advances since the 2004 classification. *J Thorac Oncol* 2015;10:1243-60.
  19. Yoshizawa A, Sumiyoshi S, Sonobe M, Kobayashi M, Fujimoto M, Kawakami F, Tsuruyama T, Travis WD, Date H, Haga H. Validation of the IASLC/ATS/ERS lung adenocarcinoma classification for prognosis and association with EGFR and KRAS gene mutations: analysis of 440 Japanese patients. *J Thorac Oncol* 2013;8:52-61.
  20. Rusch VW, Asamura H, Watanabe H, Giroux DJ, Rami-Porta R, Goldstraw P, Members of ISC. The IASLC lung cancer staging project: a proposal for a new international lymph node map in the forthcoming seventh edition of the TNM classification for lung cancer. *J Thorac Oncol* 2009;4:568-77.
  21. Bjerregaard LG, Pedersen DC, Mortensen EL, Sorensen TIA, Baker JL. Breastfeeding duration in infancy and adult risks of type 2 diabetes in a high-income country. *Matern Child Nutr* 2019;15:e12869.
  22. Haneuse S, VanderWeele TJ, Arterburn D. Using the E-value to assess the potential effect of unmeasured confounding in observational studies. *JAMA* 2019;321:602-3.
  23. Tixier F, Hatt M, Le Rest CC, Le Pogam A, Corcos L, Visvikis D. Reproducibility of tumor uptake heterogeneity characterization through textural feature analysis in 18F-FDG PET. *J Nucl Med* 2012;53:693-700.
  24. Chen B, Xia W, Wang Z, Zhao H, Li X, Liu L, Liu Y, Hu J, Fu X, Li Y, Xu Y, Liu D, Yang H, Xu L, Jiang F. Risk analyses of N2 lymph-node metastases in patients with T1 non-small cell lung cancer: a multi-center real-world

- observational study in China. *J Cancer Res Clin Oncol* 2019;145:2771-7.
25. Zhang T, Zhang JT, Li WF, Lin JT, Liu SY, Yan HH, Yang JJ, Yang XN, Wu YL, Nie Q, Zhong WZ. Visceral pleural invasion in T1 tumors ( $\leq 3$  cm), particularly T1a, in the eighth tumor-node-metastasis classification system for non-small cell lung cancer: a population-based study. *J Thorac Dis* 2019;11:2754-62.
  26. Tao H, Hayashi T, Sano F, Takahagi A, Tanaka T, Matsuda E, Okabe K. Prognostic impact of lymphovascular invasion compared with that of visceral pleural invasion in patients with pN0 non-small-cell lung cancer and a tumor diameter of 2 cm or smaller. *J Surg Res* 2013;185:250-4.
  27. Shikuma K, Menju T, Chen F, Kubo T, Muro S, Sumiyoshi S, Ohata K, Sowa T, Nakanishi T, Cho H, Neri S, Aoyama A, Sato T, Sonobe M, Date H. Is volumetric 3-dimensional computed tomography useful to predict histological tumour invasiveness? Analysis of 211 lesions of cT1N0M0 lung adenocarcinoma. *Interact Cardiovasc Thorac Surg* 2016;22:831-8.
  28. Yoshiyasu N, Kojima F, Hayashi K, Bando T. Radiomics technology for identifying early-stage lung adenocarcinomas suitable for sublobar resection. *J Thorac Cardiovasc Surg* 2021;162:477-485.e1.
  29. Heuvelmans MA, Walter JE, Vliegenthart R, van Ooijen PMA, De Bock GH, de Koning HJ, Oudkerk M. Disagreement of diameter and volume measurements for pulmonary nodule size estimation in CT lung cancer screening. *Thorax* 2018;73:779-81.
  30. Wang L, Li T, Hong J, Zhang M, Ouyang M, Zheng X, Tang K. 18F-FDG PET-based radiomics model for predicting occult lymph node metastasis in clinical N0 solid lung adenocarcinoma. *Quant Imaging Med Surg* 2021;11:215-25.
  31. Tsutani Y, Miyata Y, Nakayama H, Okumura S, Adachi S, Yoshimura M, Okada M. Prognostic significance of using solid versus whole tumor size on high-resolution computed tomography for predicting pathologic malignant grade of tumors in clinical stage IA lung adenocarcinoma: a multicenter study. *J Thorac Cardiovasc Surg* 2012;143:607-12.
  32. Jansen BHE, Yaqub M, Voortman J, Cysouw MCF, Windhorst AD, Schuit RC, Kramer GM, van den Eertwegh AJM, Schwarte LA, Hendrikse NH, Vis AN, van Moorselaar RJA, Hoekstra OS, Boellaard R, Oprea-Lager DE. Simplified methods for quantification of 18F-DCFPyL uptake in patients with prostate cancer. *J Nucl Med* 2019;60:1730-5.

**Cite this article as:** Li XF, Shi YM, Niu R, Shao XN, Wang JF, Shao XL, Zhang FF, Wang YT. Risk analysis in peripheral clinical T1 non-small cell lung cancer correlations between tumor-to-blood standardized uptake ratio on  $^{18}\text{F}$ -FDG PET-CT and primary tumor pathological invasiveness: a real-world observational study. *Quant Imaging Med Surg* 2022;12(1):159-171. doi: 10.21037/qims-21-394